EXHIBIT Z

/RESEARCH

Kinetic PCR Analysis: Real-time Monitoring of DNA Amplification Reactions

Russell Higuchi*, Carita Fockler, Gavin Dollinger[1] and Robert Watson

Roche Molecular Systems, Inc., 1145 Atlantic Ave., Alameda, CA 94501. [1]Chiron Corporation, 1400 53rd St., Emeryville, CA 94608.
*Corresponding author.

We describe a simple, quantitative assay for any amplifiable DNA sequence that uses a video camera to monitor multiple polymerase chain reactions (PCRs) simultaneously over the course of thermocycling. The video camera detects the accumulation of double-stranded DNA (dsDNA) in each PCR using the increase in the fluorescence of ethidium bromide (EtBr) that results from its binding duplex DNA. The kinetics of fluorescence accumulation during thermocycling are directly related to the starting number of DNA copies. The fewer cycles necessary to produce a detectable fluorescence, the greater the number of target sequences. Results obtained with this approach indicate that a kinetic approach to PCR analysis can quantitate DNA sensitively, selectively and over a large dynamic range. This approach also provides a means of determining the effect of different reaction conditions on the efficacy of the amplification and so can provide insight into fundamental PCR processes.

Received 9 June 1993; accepted 21 July 1993.

To facilitate its automation, any assay intended for large-scale use should be simplified as much as possible. One such simplification, a homogenous (i.e., "one-tube") approach to sequence-specific DNA detection using a fluorescent, DNA-binding dye directly in a polymerase chain reaction (PCR)[1,2] has previously been described[3]. This approach depends on the fluorescence enhancement produced when a dye such as ethidium bromide (EtBr) binds dsDNA. Since PCR produces dsDNA as the reaction proceeds, the presence of EtBr results in a net increase in fluorescence with increasing cycles of amplification. In our previous paper[3], such fluorescence increases were primarily monitored after completion of thermocycling. Such an "endpoint" analysis, as is typically done using PCR, reveals the presence or absence of target DNA but does not provide a good measure of the starting number of DNA targets. In this paper, we show that a kinetic analysis mode, in which the level of amplified DNA is continuously monitored over the course of amplification, can provide this quantitative information as well as provide information about the amplification process itself.

Previously[3], we used a bifurcated optical fiber to bring excitation illumination from a spectrofluorometer to a single PCR and to return fluorescence for measurement. In order to monitor many amplifications simultaneously, we now use a video camera to capture fluorescence images of an array of PCRs in the sample block of a thermocycler. This configuration is diagrammed in Figure 1. A computer-controlled, cooled CCD camera, as described in Sutherland et al.[4], is mounted on a copy stand with its lens focused on the surface of the thermocycler block. UV lights (302 nm) are mounted flanking the camera and directed at the block. To reduce parallax effects, the camera and light assembly is placed as far as is practical from the block. A 600 nm interference filter is placed in front of the lens to limit detection to the desired wavelength. The camera is connected to a "frame-grabber" in a desk-top computer that allows the digitized images to be saved for later manipulation.

A kinetic PCR analysis is performed by taking and saving a video image of the PCRs during each annealing/extension phase. Figure 2 shows three of many images taken during the course of six simultaneous PCRs. At the end of the run, the images are recalled and, using image-analysis software, the average intensity of emitted light from each PCR tube is determined. These fluorescence values are saved to a computer spreadsheet for analysis and graphing. A more complete description of the instrumentation and software used is being prepared (R. Watson).

Results

Continuous monitoring using a video camera. Figure 3A shows the fluorescence measured from eight amplifications monitored simultaneously during thermocycling for fifty-five

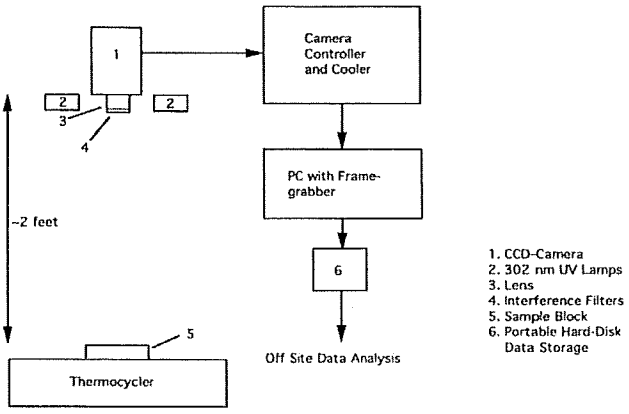

FIGURE 1. Block diagram of video camera system used to monitor amplifications in thermocycler. See Experimental Protocol for more details.

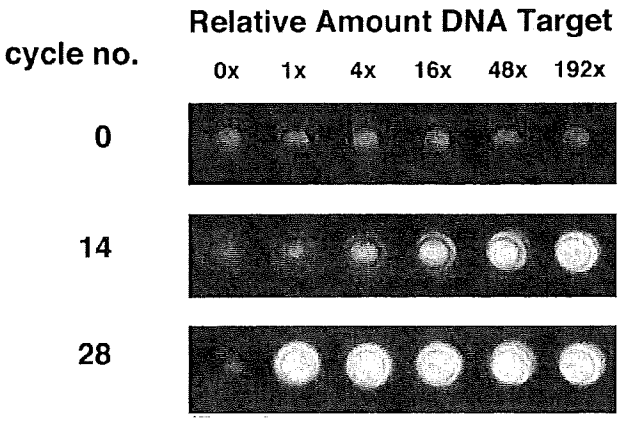

FIGURE 2. Composite of portions of video images taken using the set-up shown in Figure 1. These images are of EtBr-containing PCRs in the thermocycler block (Perkin-Elmer Model 480) and are taken looking down through the tube caps under UV (302 nm) illumination. The three images were of the same six PCRs held at the annealing/extension temperature before beginning thermocycling (cycle 0), and during the annealing/extension phase of cycles 14 and 20. Only one row of samples in the image is shown; a full block of 48 samples in a TC 480 or 96 samples in a TC 9600 can be imaged. The PCRs were initiated using a dilution series of target DNA (a 242 bp segment of HLA DQα gene[18]) at the indicated relative levels (192× = 3×10^{10} target molecules <8 ng DNA). These images demonstrate the general principle that the higher the starting amount of target DNA, the earlier the cycle at which increased fluorescence is detectable.

cycles. To assess the quantitative performance of this assay, the amplifications were initiated using a dilution series of single-stranded, HIV template DNA (see Experimental Protocol). Starting with 10^8 templates, 10-fold dilutions were made down to 10^2 templates and used with HIV-specific primers to make a 142 bp PCR product. A control amplification with no added template was also monitored. To simulate a PCR-based screen of lymphocyte DNA for integrated HIV genomes[5], all reactions contained 300 ng (40,000 cell equivalents) of human genomic DNA. Each video image was taken 20 seconds after the annealing/extension temperature was reached during the 30 second hold. The fluorescence values plotted are the average of the pixel values in the video image of each amplification tube.

As expected, the fluorescence from each reaction changes little in initial thermocycles and then rises as detectable amounts of PCR product are generated. The more starting template copies in the reaction, the earlier such a rise in fluorescence occurs. There is a considerable variance in the initial fluorescence values obtained from the different amplifications even though it is expected that these initial values should be the same (the varying amounts of single-stranded template DNA are so small that they have a negligible effect on the total fluorescence). The sources of this variation are apparently inhomogeneity of illumination, parallax, and variable attenuation of the fluorescence due to the tube caps. We have found that viewing amplifications without caps but through a vapor barrier of mineral oil or Ampliwax™ reduces, but does not eliminate, this variation.

This variation can also be seen in Figure 4, a plot of fluorescence vs. DNA concentration for known amounts of phage λ DNA. The DNA was in PCR buffer with primers and with 4 μg/ml EtBr and the measurements were made at 68°C. Each tube was imaged without its cap and through melted Ampliwax™. Fluorescence was measured for five replicate samples of each DNA concentration. The standard deviation was, on average, ±4% (as compared to ±11% for the initial values in Fig. 3A). Comparison of Figure 4 with Figure 3A also shows that it takes the fluorescence of ~50 ng of dsDNA to exceed the fluctuation in fluorescence during early cycles, suggesting that this amount of amplified DNA is the lower limit of detection of amplified DNA. Also, it is apparent that fluorescence detected in these amplifications is linearly related to the concentration of dsDNA, and that up to 4 μg of dsDNA are being made in the amplifications.

Fluorescence normalization and quantitative analysis. To compensate for measurement variation, a normalization factor for each amplification was derived which is the ratio of the average initial fluorescence of all reactions to the observed initial fluorescence of each reaction. All fluorescence values for each amplification were multiplied by this factor. This normalization (the result of which is shown in Fig. 3B) is derived from the assumption that the source of the image variation attenuates or enhances the fluorescence signal proportionately over the entire range of signal intensities. All reactions now begin at the same fluorescence and most of the reaction profiles have a regular spacing consistent with the dilution series performed. The profiles are very similar in shape and nearly parallel. The early or

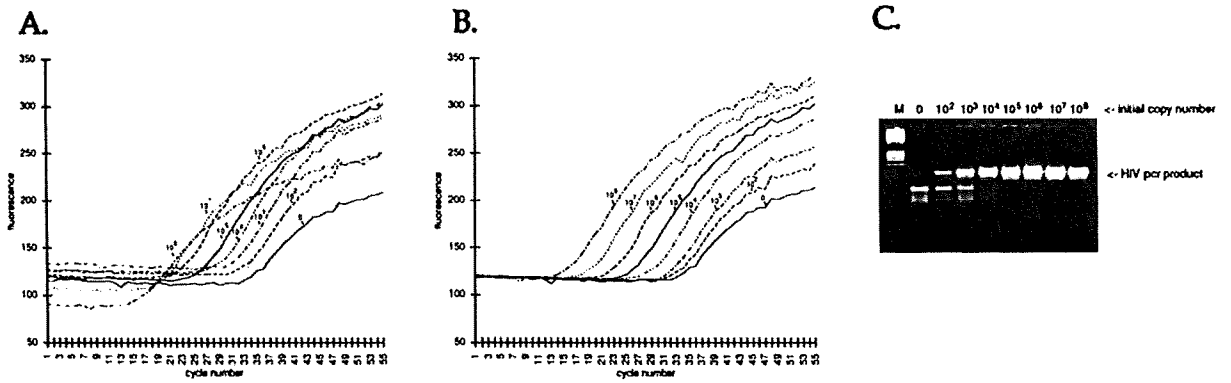

FIGURE 3. (A) "Raw data" fluorescence profiles of eight EtBr-containing PCRs that were identical except for the indicated number of HIV template molecules they contained prior to amplification. (B) Normalized fluorescence profiles of the same PCRs shown in A. (C) "Nu-Sieve" agarose gel electrophoresis of the final amplification products of the experiment in (A & B). The expected mobility of the HIV-specific amplification product (142 bp) is indicated. The marker (m) lane contains a Hae III restriction enzyme digest of φX 174 DNA. The DNA in the gel is stained with EtBr and photographed under ultraviolet light. The amount of initial target DNA is indicated for each lane.

logarithmic phase of an efficient PCR involves a doubling of the DNA copy number every cycle[2]. It is predicted that each 10-fold dilution in starting template would require 3.32 additional cycles to bring the yield of PCR product up to a given concentration. For much of the range of fluorescence levels, it can be seen by examination of Figure 3B that there are close to three cycles separating each of the dilutions except for those starting with 10^2 copies and 0 copies. It is apparent that this cycle-number-offset is persisting past the logarithmic phase of the PCRs. In contrast, the number of cycles separating the dilutions in the unnormalized data of Figure 3A vary widely.

Using the normalized data, the quantitative performance of this assay can be assessed. Figure 5 shows the linear relationship between the log of the starting number of template copies and the number of cycles it takes for the amplifications in Figure 3B to reach the arbitrarily chosen fluorescence level of 190. The line shown is regression fitted to the data points from 10^8 to 10^3 initial copies ($r^2 > .99$). The data point corresponding to 10^2 initial copies has a statistically significant deviation from this line (zero copies cannot be placed on a logarithmic plot). Besides the data point at 10^2 copies, the data point most deviant from the regression line is at 10^5, which, using the equation of the fitted line, predicts a value 13% lower than the known initial number of copies. Similar results are obtained if the fluorescence level chosen is anywhere from 125–225.

The reason for the deviation from linearity at the data point at 10^2 copies is shown by the gel electrophoresis analysis of the amplification products in Figure 3C. The specificity of the amplification is such that, starting with 10^8 down to 10^5 copies of template, the only visible product is that of the expected size. When 10^4 starting copies were used, a smaller, non-specific amplification product becomes barely visible. This product is more prominent when 10^3 copies are used, and when 10^2 copies are used, an equal amount of non-specific product and HIV-specific product are made. Only non-specific product is made in the control with no added template. Since fluorescence due to specific product is indistinguishable from that of non-specific product, the "baseline" of sensitivity of this assay is at the cycle number by which so much of non-specific product is being synthesized that any additional synthesis of specific product has little effect on the reaction profile. As long as concentration determinations are based on interpolation from a set of standards, this baseline could be at significantly more cycles than at the cycle number at which the deviation from linearity begins. In practice we have seen that sample-to-sample variation of the reaction profile at less than 10^2 templates complicates reproducible quantitation below this level (data not shown).

Effect of reaction conditions on PCR kinetics. Another application of this assay is monitoring the effect of different reaction conditions on a PCR. For example, Figure 6A shows a titration of Taq DNA polymerase. Nine replicate PCRs containing 10^8 target HIV templates were initiated using a range of Taq polymerase levels as indicated in the figure. For enzyme amounts between 1 and 10 units per reaction, fluorescence begins to be detectable in all reactions by about the same cycle. This indicates that these differences in enzyme level are having little effect on the efficiency of amplification in early cycles. Differences in the level of PCR product become apparent in later cycles, however. By cycle 50 almost twice as much DNA has been made using 10 units as compared to 1 unit. By gel electrophoresis (not shown), there is no evidence of the production of non-specific, non-HIV PCR product in these reactions. Using only 0.5 unit of Taq polymerase, there is a sudden absence of detectable product. Since PCR is a process in which DNA increases in concentration exponentially, it is perhaps not surprising that there is a threshold level of enzyme below which amplification is an apparent failure.

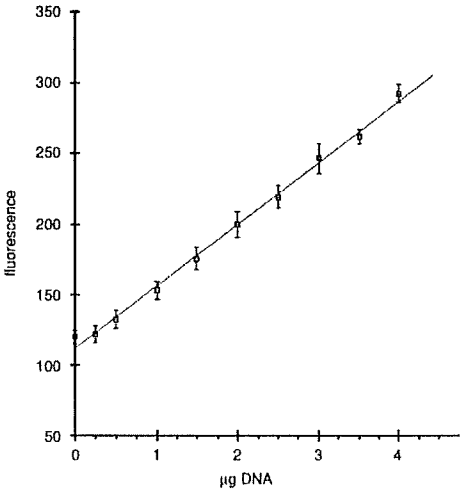

FIGURE 4. The fluorescence of λDNA solutions at different concentrations measured using the video-camera set-up in Figure 1. Five replicate samples at each concentration of DNA in PCR buffer (see Experimental Protocol) containing 4 µg/ml of EtBr, HIV specific primers (1 µm each), and no target DNA were measured at 68°C in the thermocycler. ± One standard deviation is indicated for each concentration.

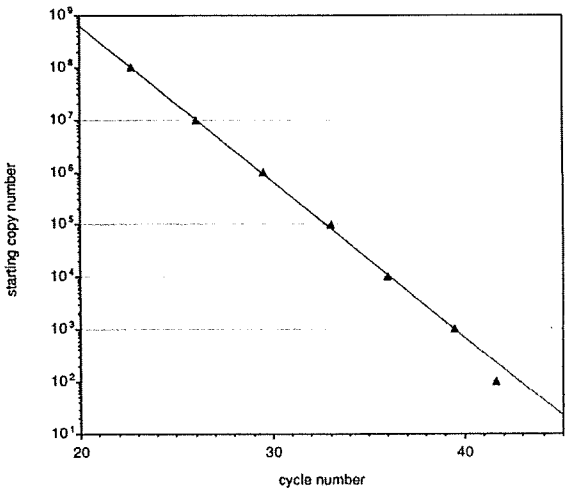

FIGURE 5. Based on the data in Figure 3B, a plot of the log of the initial template copy number vs. number of cycles it took to reach a fluorescence level = 190. The numbers of cycles can be fractional and were calculated based on a regression line fitted to the eight data points surrounding 190 in each fluorescence trace. The line in this figure is a linear regression fit to the data points from 10^8 to 10^3 copies ($r^2 > .99$).

We have also monitored the effect of changing primer concentrations on the kinetics of amplification. Figure 6B shows profiles of PCRs detecting HIV templates (10^8 initial ssDNA copies) using primer levels from 2 μM (each primer) down to 0.05 μM. A constant level of enzyme (2.5 U) was used in each PCR. Note that from 0.05 to 0.4 μM in primer concentration, the DNA level in the reaction rises to a certain level and remains constant. If these final product levels are estimated using the data in Figure 4 and assuming 10.6 pmole/μg of 142 bp PCR product, we see that for 0.05, 0.10, and 0.20 μM primer, 0.05, 0.10, and 0.20 μM product respectively, is made. At these levels, primer concentration is apparently the limiting factor on yield of product DNA. In contrast, at 0.8 μM primer concentration and above, the DNA level is continuing to rise with each

thermocycle, as in Figure 6A, and increasing amounts of primer have little effect on the profile. By comparison with the data in Figure 6A, one would conclude that these reactions are now enzyme, and not primer, limited.

The result of varying KCl concentration using the same HIV test system with 1 μM primers and 2.5 U of enzyme per 100 μl reaction are shown in Figure 6C. Taq DNA polymerase activity is greatly inhibited by high concentrations of KCl[6]. Consistent with this, at concentrations of KCl of 125 mM or greater there is no detectable PCR product. With activated salmon sperm DNA as template there is an optimum in Taq DNA polymerase activity at 50–90 mM KCl[5]. Figure 6C shows that product yield is highest at 50, 75 and 100 mM KCl with only about half as much being made at 0 mM KCl. It is possible that this difference in yield is due to low ionic strength destabilizing primer annealing, although this explanation is not consistent with the fact that the efficiency of amplification using 0 mM KCl is nearly the same as those at 50–100 mM KCl until about cycle 20. Only in later cycles does product yield falls off, similar to the results obtained with less polymerase in Figure 6A. If primer annealing were destabilized, one would expect that amplification efficiency would be diminished for all cycles.

Lastly, a known inhibitor of PCR, hematin[7], was added to PCRs at various concentrations. Hematin was added to the same HIV test system used before, except that a primer concentration of 0.2 μM was used. As shown in Figure 6D, at hematin concentrations of 0.2 μM and greater, no detectable DNA product is obtained. At 0.1 μM, the detection of product is delayed by 3–4 cycles, suggesting that, in contrast with the results obtained with 0 mM KCl or reduced enzyme, the efficiency of amplification is being detrimentally affected both in early and late amplification cycles. This difference in reaction profiles suggests that partially inhibited PCRs can be distinguished from uninhibited reactions.

Discussion

Kinetic PCR analysis permits the sensitive, quantitative detection of specific DNA sequences over a wide dynamic range. This detection is "homogeneous" in that, once amplification is begun, tubes need not be opened for sampling. This reduces the amount of labor required, simplifies the process and reduces the risk of PCR product "carryover" contamination[8] into subsequent reactions. Kinetic PCR analysis also provides a simple means of monitoring the effect of different PCR conditions.

A number of other assays have been described which quantitate the number of starting DNA templates in a PCR[9–11]. Some involve the measurement of PCR product at the end of thermocycling and relating this level to the starting DNA concentration. Others involve the use of a competitor amplification product whose template is added at known concentration to the reaction mixture before thermocycling. In competitor-product protocols, an aliquot of the amplification is examined by gel- electrophoresis. The relative amount of target-specific and competitor PCR product is measured; this ratio is used to calculate the starting number of target templates. The larger the ratio of target-specific product to competitor-specific product, the higher the starting DNA concentration.

In addition to requiring "downstream" processing, such as hybridization or gel electrophoresis, these other assays are more limited in dynamic range. In competitor assays, the sensitivity to template concentration differences is compromised when either the target or added competitor DNA is greatly in excess. The dynamic range of assays that measure the amount of end product can also be limited in that, at the chosen number of cycles, some reactions may have reached a "plateau" level of product. Differ-

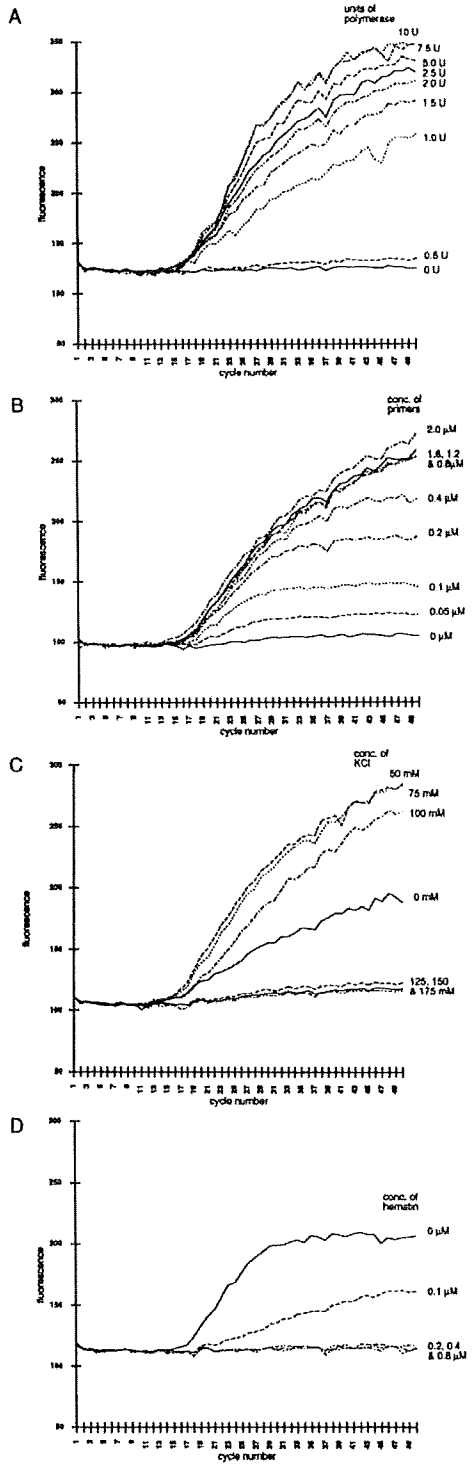

FIGURE 6. (A) Effect of polymerase concentration. Fluorescence profiles of nine PCRs, each begun with 10^9 copies of HIV, ssDNA template but differing only in the amount of Taq DNA polymerase. HIV-specific primers were at 1.0 µM and KCl was at 50 mM. (B) Effect of primer concentration. Similar to (A), but all PCRs had 2.5 U of Taq DNA polymerase and 50 mM KCl and differed only in the concentration of HIV-specific primers used. (C) Effect of KCl concentration. Similar to (A and B), but all PCRs had 2.5 U of polymerase and 1.0 µM HIV-specific primers but differed only in the concentration of KCl used. (D) Effect of a known inhibitor. Hematin was added at the indicated levels to PCRs similar to those in (A–C). Taq polymerase (2.5 U), 0.2 µM primers, and 50 mM KCl were used in all reactions.

ences in starting template levels in these reactions are therefore not well reflected. Furthermore, small differences in the measured amount of product due to variable reaction conditions, variations in sampling, or the presence of inhibitors, result in widely varying estimates of the starting template concentration.

The ability to monitor in real-time the level of dsDNA being made can help circumvent these problems. As shown in this paper, a dynamic range of at least six orders of magnitude is possible with kinetic PCR analysis, simultaneous with sensitivity to as few as 100 ssDNA templates in the background of 40,000 cell-equivalents of complex genomic DNA. Also, in our experience, template quantitation using kinetic PCR analysis is less sensitive to measurement variations than quantitation based upon of product level at the end of thermocycling. Furthermore, as shown in Figure 6D, instances of partial inhibition of PCR, which can very adversely affect accurate quantitation, may be detected by examination of the reaction profile, so that these samples can be repurified and tested again. Instances of total inhibition can also be distinguished from truly negative samples since given enough cycles, even PCRs without target DNA will produce fluorescence that is due to non-specific amplification products. If such products are not seen by the expected cycle, the presence of inhibitors can be inferred.

Optimization of PCR conditions has been done previously by measuring the effect of different conditions on the final yield and specificity of PCR product. In order to obtain information throughout amplification, many replicate samples would need to be removed from the thermocycler and analyzed by gel electrophoresis as a function of cycle number. Using real-time monitoring, one amplification suffices to provide data points at all cycles at which product is detectable. As shown here, this data can help ascertain when in amplification the change in condition is exerting its effect. Such information will help to further optimize the yield and efficiency of amplification for specific applications.

We are working to improve kinetic PCR analysis through improvements in instrumentation, signal generation[13] and by increasing the specificity and reproducibility of PCR. For example, we are automating the collection of the sample images and their quantitation. And although the normalization procedure we have described here can compensate, we wish to further minimize sample-to-sample fluorescence variation. This may involve the use of alternative illumination and/or detection formats as well changes in the composition and/or structure of the amplification vessel. We are also testing alternative dyes and intercalators[12] and alternative strategies of detection using optically active probes based on the 5′ → 3′ exonuclease activity of Taq DNA polymerase[13]. We are working on procedures that may help increase the specificity of a PCR, including a one-tube, nested-primer approach (Higuchi and Erlich, manuscript in prep.). Lastly, we are trying to reduce the "primer-dimer" artifact[14], which may improve reproducibility of the reaction profile at extremely low levels of target DNA.

Experimental Protocol

HIV kinetic PCR analysis of sequences. PCRs were set up in 100 μl volumes containing 10 mM Tris-HCl, pH 8.3; 50 mM KCl; 3 mM $MgCl_2$; 2.5 U of Taq DNA polymerase (Perkin-Elmer, Norwalk, CT); 100 μM each dNTP (Promega Corp., Madison, WI); 4 μg/ml of Ethidium Bromide (Bio Rad, Richmond, CA); 100 pmole each of HIV specific (gag region) oligonucleotide primers SK145 and SK431[15,16] (Perkin Elmer, Norwalk, CT) and 300 ng of human placental DNA (Sigma, St. Louis, MO). A M13 subclone of the HIV *gag* region[17] was used as template at the copy-numbers indicated in Figure 3. When caps were not used, either mineral oil or Ampliwax™ (Perkin-Elmer, Norwalk, CT) was used as a vapor barrier. Thermocycling proceeded for 55 cycles in a GeneAmp PCR System 9600 thermocycler (Perkin-Elmer, Norwalk, CT) with a 2 temperature program of 94°C for 15 sec. denaturing and 68°C for 30 sec. annealing/extension. To provide a "hot-start"[14] an initial hold at 75°C was used during which the $MgCl_2$ was added (in a 12 μl volume) after the samples had reached this temperature. Video images for each thermocycle were taken 20 sec. into the 30 sec. hold at the annealing temperature. To allow imaging, the heated block cover was not used. For the analysis of different PCR conditions, HIV-specific PCRs were set up as described above, except without human genomic DNA and with 10^8 copies of the cloned M13 HIV template. The conditions were varied as described in Figure 6.

Instrumentation and software. The video camera used is a STAR1 system from Photometrics (Tuscon, Arizona). It uses a thermoelectrically cooled 384 × 560 CCD array with a 12 bit A/D controller. Exposure times can be varied to change sensitivity to the fluorescence being detected. Typically exposures of 1 sec. were used with virtually no thermal or random noise. Illumination is provided by two Chroma-Vue, 302 nm, mid-range U.V. lamps from U.V. products (San Gabriel, CA). A PC Vision Plus frame grabber board (Imaging Technology, Inc., Woburn, Mass.) and Jandel Scientific's (San Raphael, CA) JAVA image analysis software was used to quantitate areas of interest in the captured image. Bernoulli 90 MB removable disks from IOMEGA Corp. were used for image storage and as a means of providing unlimited storage. Data analysis was done using Microsoft Excel 4.0.

Acknowledgments

We thank Henry Erlich, David Gelfand, John Sninsky, and Tom White for their support and advice, Kathy Ordoñez for the name, kinetic PCR assay, and Karen Beranek for help in preparing this manuscript.

References

1. Mullis, K., Faloona, F., Scharf, S., Saiki, R., Horn, G. and Erlich, H. 1986. Specific enzymatic amplification of DNA *in vitro*: The polymerase chain reaction. Cold Spring Harb. Symp. Quant. Biol. **51**:263–273.
2. Saiki, R. K., Gelfand, D. H., Stoffel, S., Scharf, S. J., Higuchi, R., Horn, G. T., Mullis, K. B. and Erlich, H. A. 1988. Primer-Directed Enzymatic Amplification of DNA with a Thermostable DNA Polymerase. Science **239**:487–491.
3. Higuchi, R., Dollinger, G., Walsh, P. S, and Griffith, R. 1992. Simultaneous amplification and detection of specific DNA sequences. Bio/Technology **10**:413–417.
4. Sutherland, J. C., Sutherland, B. M., Emrick, A., Monteleone, D. C., Ribeiro, E. A., Trunk, J., Son, M., Serwer, P., Poddar, S. K. and Maniloff, J. 1991. Quantitative electronic imaging of gel fluorescence with CCD cameras: Applications in molecular biology. Biotechniques **10**:492–497.
5. Kwok, S. Y., Mack, D. H., Mullis, K. B., Poiesz, B. J., Ehrlich, G. D., Blair, D. and Friedman-Kien, A. S. 1987. Identification of human immunodeficiency virus sequences by using *in vitro* enzymatic amplification and oligomer cleavage detection. J. Virol. **61**:1690–1694.
6. Lawyer, F. C., Stoffel, S., Saiki, R. K., Chang, S., Landre, P., Abramson, R. and Gelfand, D. H. 1993. High-level expression, purification, and enzymatic characterization of full-length *Thermus aquaticus* DNA polymerase and a truncated form deficient in 5′ to 3′ exonuclease activity. PCR Joumal. *In press*.
7. Walsh, P. S., Metzger, D. A. and Higuchi, R. 1991. Chelex 100 as a medium for simple extraction of DNA for PCR-based typing from forensic material. Biotechniques **10**:506–513.
8. Higuchi, R. and Kwok, S. 1989. Avoiding false positives with PCR. Nature **339**:237–238.
9. Piatak, Jr. M., Saag, M. S., Yang, L. C., Clark, S. J., Kappes, J. C., Luk, K.-C., Hahn, B. H., Shaw, G. M. and Lifson, J. D. 1993. High levels of HIV-1 plasma during all stages of infection determined by competitive PCR. Science **259**:1749–1754.
10. McCarrey, J. R., Dilworth, D. D. and Sharp, R. M. 1992. Semiquantitative analysis of X-linked gene expression during spermatogenesis in the mouse: Ethidium-bromide staining of RT-PCR products. Genet. Anal. Tech. Appl. **9**:117–123.
11. Gilliland, G., Perrin, S., Blanchard, K. and Bunn, H. F. 1990. Analysis of cytokine mRNA and DNA: Detection and quantitation by competitive polymerase chain reaction. Proc. Natl. Acad. Sci. **87**:2725–2729.
12. Rye, H. S., Yue, S., Wemmer, D. E., Quesada, M.A ., Haugland, R. P., Mathies, R. A. and Glazer, A. N. 1992. Stable florescent complexes of double-stranded DNA with bis-intercalating asymmetric czanimol dyes: properties and applications. Nucl. Acids Res. **20**:2803–2812.
13. Holland, P. M., Abramson, R. D., Watson, R. and Gelfand, D. H. 1991. Detection of specific polymerase chain reaction product by utilizing the 5′→3′ exonuclease activity of *Thermus aquaticus* DNA polymerase. Proc. Natl. Acad. Sci. **88**:7276–7280.
14. Chou, Q., Russell, M., Birch, D. E., Raymond, J. and Bloch, W. 1992. Prevention of pre-PCR mis-priming and primer dimerization improves low-copy-number simplifications. Nucl. Acids Res. **20**:1717–1723.
15. Kwok, S., Kellogg, D. E., McKinney, N., Spasic, D., Goda, L., Levenson, C. and Sninsky, J. J. 1990. Effects of primer-template mismatches on the polymerase chain reaction: Human immunodeficiency virus type 1 model studies. Nucl. Acids Res. **18**:999–1005.
16. Jackson, J. B., Ndugwa, C., Mmiro, F., Kataaha, P., Guay, L., Dragon, E. A., Goldfarb, J. and Olness, K. 1991. Non-isotopic polymerase chain reaction methods for the detection of HIV-1 in Ugandan mothers and infants. AIDS **5**:1463–1467.
17. Sanchez-Pescador, R., Power, M. D., Barr, P. J., Steimer, K. S., Stempien, M. M., Brown-Shimer, S. L., Gee, W. W., Renard, A., Randolph, A., Levy, J. A., Dina, D. and Luciw, P. A. 1985. Nucleotide sequence and expression of an AIDS-associated retrovirus (ARV-2). Science **227**:484–492.
18. Horn, G. T., Bugawan, T. L., Long, C. M. and Erlich, H. A. 1988. Allelic sequence variation of the HLA-DQα loci, relationship to serology and to insulin-dependent diabetes susceptibility. Proc. Natl. Acad. Sci. **85**:3504–3508.